Available online at www.sciencedirect.com

ScienceDirect

Energy Procedia 114 (2017) 6730 – 6740

Energy Procedia

13th International Conference on Greenhouse Gas Control Technologies, GHGT-13, 14-18 November 2016, Lausanne, Switzerland

Towards a Thorough Validation of Simulation Tools for CO_2 Pipeline Transport

Michael Drescher[a]*, Adil Fahmi[a], Peder Aursand[b], Morten Hammer[b], Halvor Lund[b], Jacob Stang[b], Anders Austegard[b]

[a]*Statoil ASA, Research & Technology, NO-7005 Trondheim, Norway*
[b]*SINTEF Energy Research, NO-7491 Trondheim, Norway*

Abstract

In this work the Schlumberger flow assurance tool OLGA and SINTEF Energy Research in-house CFD tool are assessed for their ability to describe depressurization behaviour of CO_2 pipelines. For this purpose, three full-bore experimental depressurization tests with pure CO_2 have been performed at the Statoil's R&D center in Trondheim, Norway.

Simulations results are in general agreement with the experiments with the exception of the behaviour at the innermost position of the where OLGA predicts significantly lower temperatures, and SINTEF tool over-estimate the temperature. Both models predict liquid dry-out time with an error of a few seconds.

The simulation results are sensitive to the pipe outer heat transfer coefficient, used between the pipe surface and the ambient humid air. Reduction of the uncertainty in the heat-flux to the pipe is identified as a key factor for further validation.

Peer-review under responsibility of the organizing committee of GHGT-13.

Keywords: CO_2; experiments; simulations; depressurization; pipeline

* Corresponding author. Tel.: +47 97003339.
E-mail address: midr@statoil.com

Peer-review under responsibility of the organizing committee of GHGT-13.
doi:10.1016/j.egypro.2017.03.1805

1. Introduction

Rolling out carbon capture and storage (CCS) at a large scale requires significant technology verification in all parts of the CCS value chain: Capture, transport, injection and storage. Flow assurance simulation tools are used in pipeline design in order to estimate pressure and temperature ratings. Moreover, they are used in order to develop procedures for optimal and safe CO_2 transport operations including start-up, shut-in and depressurization. Therefore, it is critical to be aware of the capabilities and limitations of CO_2 flow assurance tools. This was also pointed out by de Koeijer for the case of CO_2 well flow [1].

CO_2 is normally transported through pipelines in a liquid or dense phase at high pressure. Depressurization of pipelines can occur during planned blow-down operations, maintenance or undesirable accidents. When designing pipelines and developing procedures for pipeline operations, the minimum temperature encountered in the pipeline is the key parameter that can lead to steel brittleness and dry ice formation.

To develop and validate flow models for depressurization of CO_2 pipelines, there is a need for experimental data. Recently reviewed available experimental depressurization data in the literature, categorized the data based on the experimental emphasis [2]. Some experiments were only interested in the initial wave propagation, while others focused on the temperature profile after the initial rarefaction wave. The DNV-GL [3] experiments are the only experiments published for pure CO_2 where accurate temperature measurements are included.

In this work, depressurization experiments have been executed with pure liquid CO_2. To illustrate the predictive capabilities of state-of-the-art flow models, the experimental results are compared with simulation results from two flow assurance tools: Schlumberger's OLGA software and SINTEF Energy Research in-house CFD tool. The paper will present and discuss the measured and simulated results for pressure and temperature during depressurization. The focus is on the flow dynamics after the initial pressure wave.

2. Test facility

The horizontal flow circuit of the CO_2 transport test facility at Statoil's R&D center in Trondheim (Norway) was used to perform the experiments. The horizontal flow circuit consists of a test section of a 140 m long horizontal stainless steel tube with an inner diameter of 10 mm and an outer diameter of 12 mm. At approximately 0 m, 50 m, 100 m and 139 meters, pressure and temperature sensors are installed to monitor the pressure and temperature development under depressurization, as shown in Figure 1. Further details are found Drescher et al. [4].

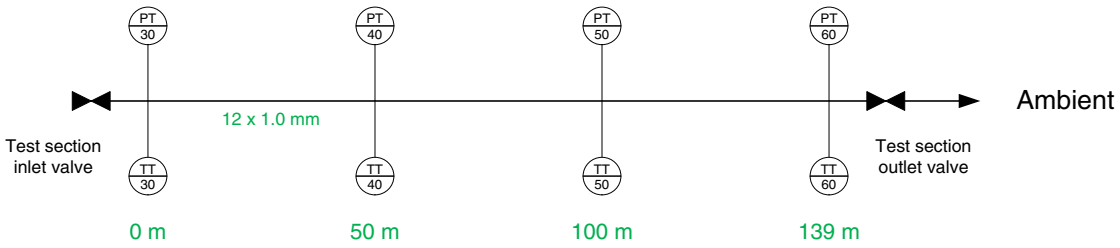

Figure 1: Set-up of the horizontal flow circuit.

3. Experimental investigations

Depressurization experiments with pure CO_2 were carried out to investigate the pressure and temperature development. The initial condition was 120 bara pressure and temperature, which varied from 15 to 25 °C. The list of depressurization tests is shown in Table 1.

To achieve the desired test pressure, the gas was compressed using an oil free gas booster. The temperature of the fluid was controlled by adjusting the ambient temperature of the test facility. After the pressure and temperature had equalized inside the test section, the high-speed logging was started quickly followed by manually opening the test-section outlet valve.

Table 1: List of depressurization tests.

Test	Initial pressure (bara)	Initial temperature (°C)	Ambient temperature (°C)
1	119.9	20.1	21.8
2	119.8	24.9	25.0
3	120.0	14.8	14.3

4. Simulation models

4.1. Ambient heat transfer

The overall heat transfer number (h(W/m^2/K)) from the surrounding air to the cold pipe surface is comprised of contributions from convection of the air (h_C) due to installed fans, radiation (h_R) and condensation or evaporation of water (h_W) on the pipe surface,

$$h = h_C + h_R + h_W.$$

The heat transfer from convection of the air is described using a standard Nusselt (Nu) number correlation [5],

$$\mathrm{Nu} = \mathrm{C} \cdot \mathrm{Re}^n \cdot \mathrm{Pr}^{1/3},$$

where n and C depend on the Reynolds (Re) number. The definition of the Nusselt, Reynolds and Prandtl numbers is as follows,

$$\mathrm{Nu} = \frac{h_C D_O}{k}, \mathrm{Re} = \frac{\rho u D_O}{\mu}, \mathrm{Pr} = \frac{C_P \mu}{k},$$

where D_O is the outer diameter, k is the thermal conductivity, μ the dynamic viscosity, ρ the density, u the velocity and Cp the heat capacity.

The heat transfer due to radiation is described using the Stefan–Boltzmann law,

$$h_R = \frac{\sigma \epsilon (T_{\mathrm{Amb}} - T_s)^4}{T_{\mathrm{Amb}} - T_s},$$

where, σ is the Stefan–Boltzmann constant, ϵ is the pipe emissivity factor, T_{Amb} is the air temperature, and T_S is the wall surface temperature.

The heat transfer due to condensation or de-sublimation is described using a mass transfer analogy. The Sherwood number is then calculated from the Nusselt number as follows,

$$\mathrm{Sh} = \frac{h_m D_o}{D_{AB}} = \mathrm{Sh}(\mathrm{Re}, \mathrm{Sc}) = \mathrm{Nu}(\mathrm{Re},\mathrm{Sc}),$$

where D_{AB} is the diffusion coefficient, h_m is the convective mass transfer rate, and Sc is the Schmidt number given as

$$\mathrm{Sc} = \frac{\mu}{\rho D_{AB}}.$$

The mass transfer through the boundary layer is then given by h_m and the water concentration difference between the surface and the bulk of the air. The concentrations are found from the saturation pressure of water or ice. Given the enthalpy of evaporation and sublimation, the heat (q_W) associated with water condensing or freezing on the surface is known. The heat transfer is then known as,

$$h_W = \frac{q_W}{T_{\mathrm{Amb}} - T_s}.$$

Heat resistance through water or ice on the wall surface is neglected. The possible effect of condensation in the boundary layer is also neglected.

The overall heat transfer coefficient will depend mainly on the air velocity, the humidity of the air, the wall surface temperature and the bulk air temperature. The wall surface temperature is predicted by the CFD models, and air temperature was measured. The humidity and the average air velocity has not been measured and must be estimated. The air velocity is estimated to be in the range 1-2 m/s, and the humidity in the range between 54-75%.

How the heat transfer coefficient depends on these parameters is visualized in Figure 2. At high surface temperatures the heat transfer number is approximately constant, but when lowering the temperature, the air becomes saturated with water and the heat transfer coefficient increases very fast. At 0 ° C, ice starts to form, and there is a jump in the heat transfer number.

Based on these results, an average heat transfer number of 55 W/m^2/K is used in the simulations.

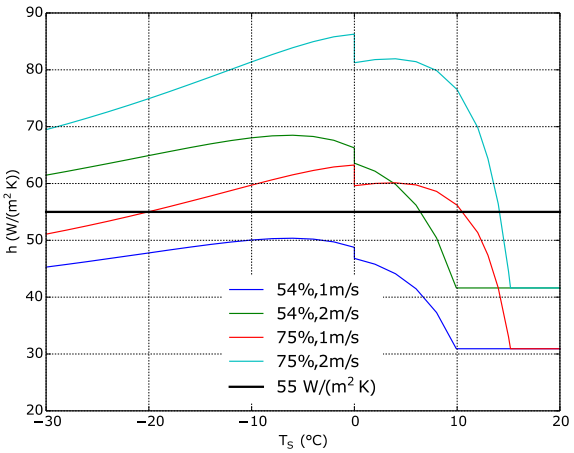

Figure 2: Overall heat transfer number as a function of wall surface temperature.

4.2. Initial and boundary conditions

Average values of temperature and pressure from the four sensors are used to define the initial state of the pipe before depressurization. The ambient temperature is measured. See Table 1 for initial state and ambient temperature. A constant pressure of 1 atm is specified at the outlet. The inlet is closed.

4.3. The OLGA model

The commercial OLGA software is one of the most used flow assurance tools for pipelines encountering two (gas-oil) or three phase flow (gas-oil-water). In addition to being a design tool for steady state friction and holdup, it is a transient simulator capable of simulating pipeline depressurisation. As one of the few available commercial tools for

CO_2 pipeline depressurization, it is of interest to see how well the model matches experimental results for full-bore depressurization.

OLGA has been extended from its initial purpose of oil and gas flow towards pure CO_2 flow. Originally, OLGA relied on a numerical scheme, where the energy conservation was transformed to a temperature equation, under the assumption of full thermodynamic equilibrium. This proved difficult when the fluid enthalpy became discontinues in temperature at the saturation line for pure fluids [6]. To overcome this issue, a non-equilibrium approach relaxing the phase transition is applied. CO_2 flow in OLGA has been validated with steady state hold-up and friction measurements, but the capabilities for fast depressurization are less documented.

Single component module

The present simulations were performed utilizing the single component module for CO_2. For a single component fluid, phase changes take place on the saturation line in the phase diagram. In equilibrium, a mix of liquid and vapor can only exist on the saturation line as opposed to the larger two-phase area resulting from a multi component fluid. Since standard OLGA uses a temperature equation, and relies on a PT-flash when computing the phase distribution, numerical instabilities occur when the saturation line is crossed for single component fluids. The single component functionality handles these numerical problems using a kinetic approach to consider the available energy whenever phase changes occur. It is ensured that the fluid stays on the saturation line until enough energy has been transferred to evaporate/condense the fluid numerical smoothing of the fluid properties close to the critical point is applied to avoid simulation instabilities.

Pure CO_2 properties

The fluid property equations are time consuming to solve and are therefore used only at the start of a simulation. A table of fluid properties is generated, and OLGA interpolates within this table during the simulation to find the properties at the current flow conditions. Note that the OLGA simulation results will not be valid if the dry ice region is entered.

Heat transfer calculations

In OLGA, it is always assumed that the gas and liquid phases have the same temperature. Heat flux through the pipe wall layers is calculated based on user-defined thermal conductivities, specific heat capacities and densities for each wall layer and assuming that radial heat conduction through the concentric walls is the dominating phenomenon. Heat transfer due to natural convection in the axial direction of the pipe is in most cases small compared to the heat that is being exchanged with the pipe wall and the heat that is transported with the fluid if there is flow in the pipe. However, natural convection in the axial direction may affect the temperature profile along a pipe geometry when the temperature gradient has the same direction as the gravity, particularly in a vertical riser or a well during a shut-in period. This is not taken into account in the simulations.

The heat transfer from the fluid to the wall and through the wall is calculated by OLGA based on the flow conditions and the thermophysical properties of the fluid and the wall material. At the outside pipe wall surface, a heat transfer coefficient of 55 W/m^2K is specified. The ambient temperature is case dependent.

4.4. The SINTEF CFD framework

A CFD framework for fast transient flow and fracture propagation control in CO_2 pipelines, have been developed and validated against several sets of experimental data. For pure CO_2 the model framework applies full thermodynamic equilibrium, and extends the Span-Wagner [7] thermodynamic fluid model using the Gibbs free energy function by Jäger and Span [8] to describe dry ice. The model supports full equilibrium of solid-liquid-vapour. Even if there is no solid inside the pipeline during the simulation, dry ice might be present and effecting the flow as the fluid chokes at the pipe outlet. The most accurate viscosity correlation available for pure CO_2, Vesovic et

al. [9], is used. The same applies for the thermal conductivity correlation by Fenghour and Wakeman [10]. Surface tension of CO_2 is accurately calculated using the correlation due to Rathjen and Straub [11]. Direct calls to the thermophysical models are employed during the simulation.

The framework supports several flow models, but since the flow is highly turbulent, a homogeneous equilibrium model (HEM) approach has been selected for calculating the full-bore depressurization. Heat transfer to the outer pipe surface and through the pipe wall is handled in a similar manner as in OLGA. The fluid model and the heat transfer model used is extensively documented in earlier work [12].

Munkejord et al. [2] simulated the full-bore depressurization experiments of DNV-GL [3]. Pure CO_2 was depressurized from a 200m long, OD 50mm pipeline. Due to pipe insulation, the temperatures of the pipeline dropped below the triple point temperature, and dry ice was formed. The model successfully predicted the formation of solid CO_2. The framework has also been applied to simulate full-bore depressurization of CO_2-N_2 mixtures, see Drescher et al. [4] and Munkejord and Hammer [12].

The modelling framework has been validated for prediction of running ductile fracture by Aursand et al. [13]. Coupling the fluid CFD framework to a solid structure finite element model, running ductile fracture propagation in a pure CO_2 pipeline was successfully simulated.

As for OLGA, the outer heat transfer coefficient is a parameter that needs to be estimated. A constant value of 55 W/(m^2 K) is used for heat transfer to the ambient.

5. OLGA simulation results

5.1. Representative case: Test 1

Test 1 will be discussed as a representative case for depressurization. Afterwards, experimental and OLGA pressure and temperature profiles will be presented.

Figure 3 shows experimental and OLGA pressure and temperature profiles at the four sensor locations. The general trend is acceptable for TT40, TT50 and TT60 positions. Predicted minimum temperatures (their occurrences and values) are close to experimental results with the largest gap between experiment and simulation found at position TT50: 4°C and 3s. The gap between predicted and experimental temperatures becomes larger after the minimum temperature is reached, at this minimum all the liquid has boiled-off.

Predicted temperature at position TT30 is very different from the experimental value. At time t=50s, OLGA predicts a very low temperature of -60°C while the sensor measures -20°C only. The reason seems to be that when all the liquid has boiled off at TT30 position in the experiment, there is still liquid CO_2 left in the simulation. Since the pressure is still going down and since the boiling liquid follows the saturation line, the result is that the temperature in the simulation continues to go down after the experimental temperature has leveled off.

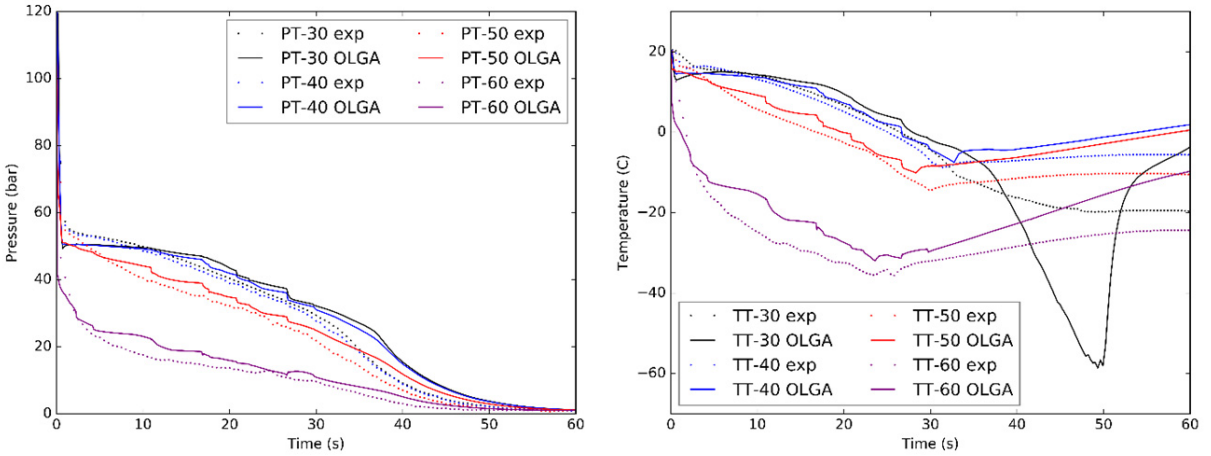

Figure 3: Experimental and OLGA pressure and temperature profiles for test 1.

Initially, the pipe contains 9.5 kg of liquid CO_2. At time t=40s, there remains 18 g of liquid located at position TT30, with a temperature of -20°C and a pressure of 15.5 bara (see Figure 3). OLGA pressure-temperature P-T curves (see Figure 4, left) show that the boil-off of these last droplets follows the saturation line until the temperature is -60°C and the pressure is 4 bara. This boil-off last 10s from t=40s until t=50s. When there is only gas at position TT30 the temperature starts to increase. Experimental results (see Figure 4, right) describe a different mechanism. The pressure-temperature curve at TT30 leaves the saturation line at a temperature of -10°C, and the temperature continues to drop until -20°C, and thereafter it starts to increase. This behavior at TT30 is rather unexpected, and does not follow the P-T trends observed at positions TT40, 50 and 60. At these positions, the temperature starts to increase immediately when the P-T curve leaves the saturation line, which means that all the liquid has boiled-off and the local gas phase starts to warm-up.

For the time being, the experimental behavior at TT30 is not fully understood. Further work is needed: Re-running the experiment, closely monitoring the sensor behavior, and visually confirming (using a see-glass) the dry-out time.

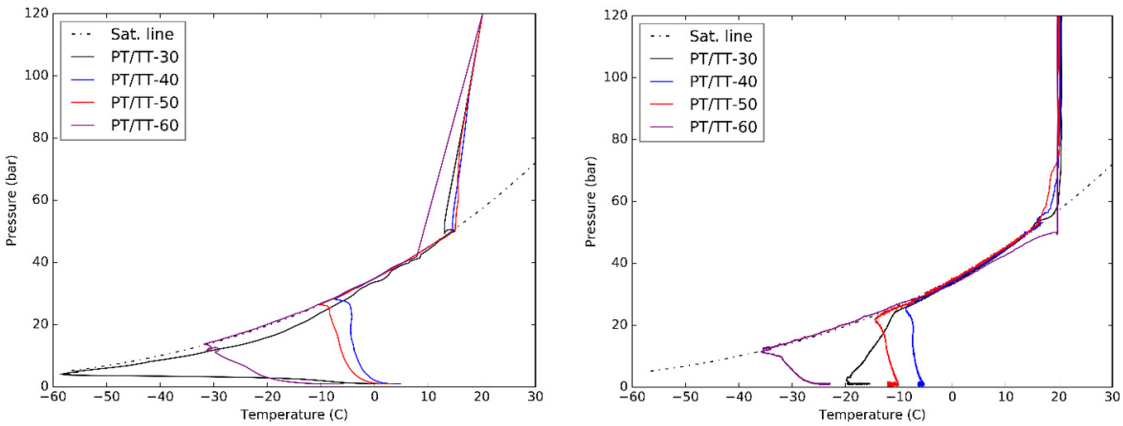

Figure 4: Pressure and temperature trajectory for the four sensors in test 1 from OLGA on the left, and from experiments on the right.

5.2. Results of tests 2 and 3

Tests 2 and 3 follow the same trend discussed for test 1. The gap between experimental and calculated temperatures at TT40 and 50 is larger for test 3 compared with tests 1 and 2.

For the pressure profiles, test 1 shows a better match between experiment and simulation compared with tests 2 and 3. Moreover, the lowest gap is observed at location TT60.

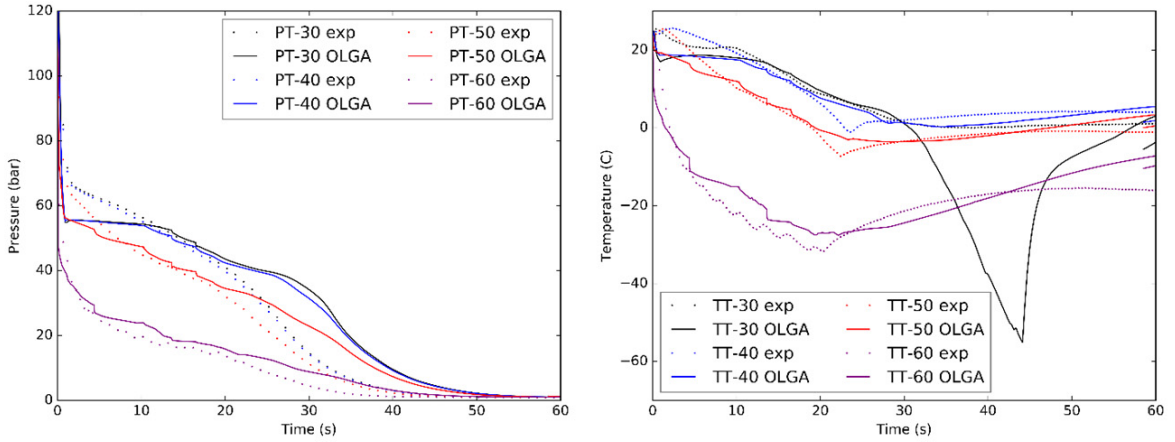

Figure 5: Experimental and OLGA pressure and temperature profiles for test 2.

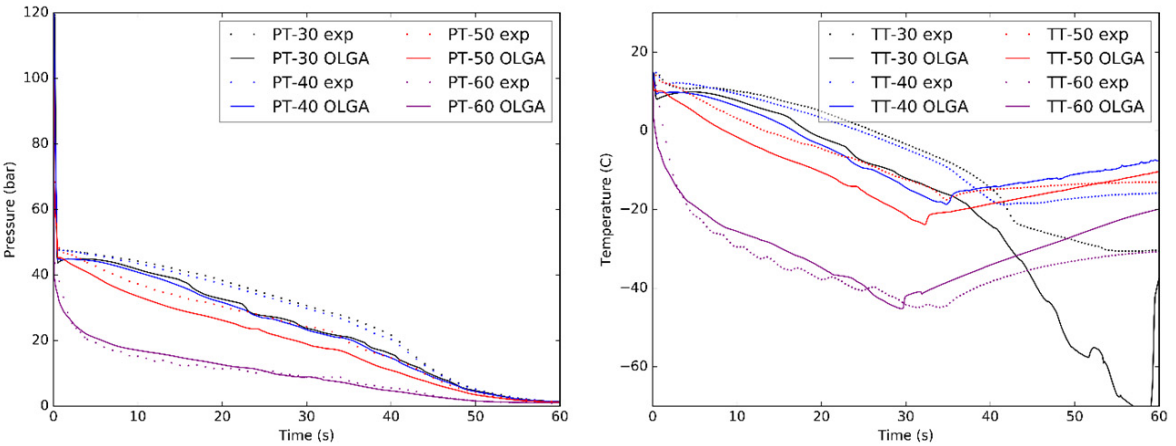

Figure 6: Experimental and OLGA pressure and temperature profiles for test 3.

6. SINTEF simulation results

In the computations, a grid of 600 cells and a CFL number of 0.85 were used. Figures 7, 8 and 9 show the measured and computed evolution of pressure and temperature for depressurization tests 1, 2, and 3, respectively. When the valve is opened the pressure in the entire pipe is rapidly reduced (within 1 s) to about half the initial pressure. From this point, the depressurization is limited by choked flow and is significantly slowed. The pipe empties slowly in the course of the subsequent 40-60 seconds. The temperature evolution shows a pattern of rapid cooling, yielding temperatures as low as -50°C closest to the valve.

Overall, there is a reasonable agreement between the pressure in experiments and simulations. The best match is found in test 2, where both the pressure and the time of dry-out are well predicted. In tests 1 and 3 the time before dry-out is under-estimated. For temperature profiles, the simulations underestimate the lowest occurring temperature near the opening (TT60) by about 10 degrees. Temperatures at the other locations have a better match until the time of dry-out. Thereafter, the simulations seem to slightly over-estimate the heat transfer from the surroundings, since the simulated temperatures rise quicker than the experimental ones, especially for tests 1 and 3.

In addition, the simulated temperature at the innermost position (TT30) has an S-curve shape not seen in the experiments.

The discrepancy between experimental and simulation temperatures at the innermost position may be explained by an evaporating liquid plug at this position. The model employed in the simulations does not include phase slip, which means that both phases move with the same velocity. This may enhance liquid removal from the pipe and makes the occurrence of dry-out much earlier than the experiment.

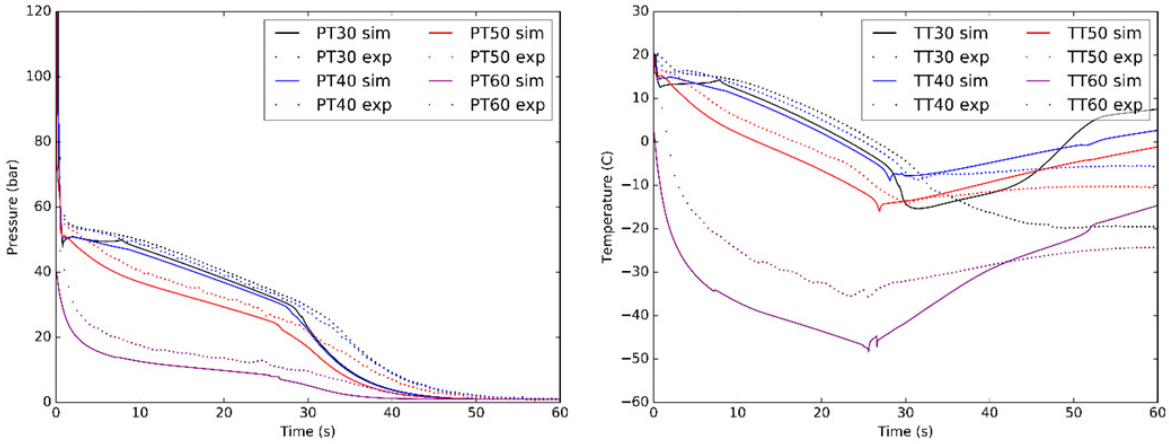

Figure 7: Experimental and SINTEF code pressure and temperature profiles for test 1.

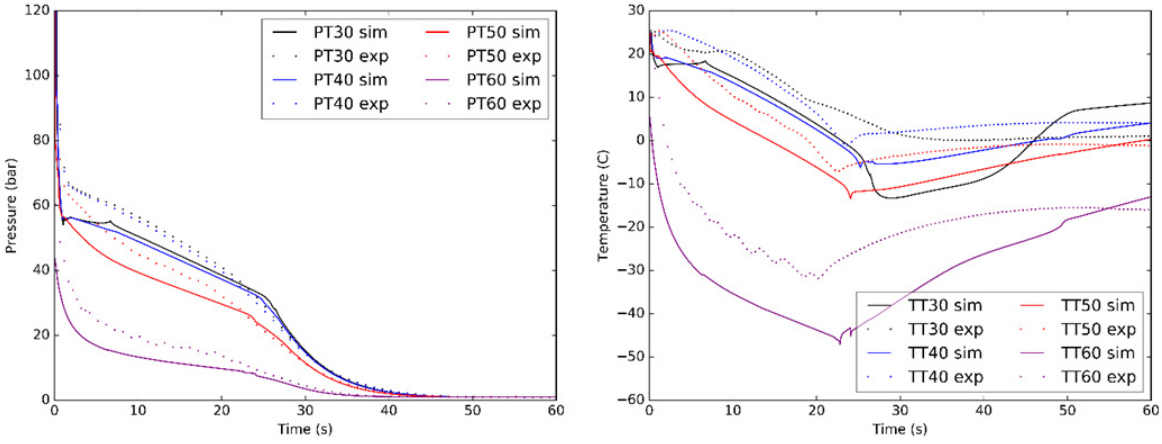

Figure 8: Experimental and SINTEF code pressure and temperature profiles for test 2.

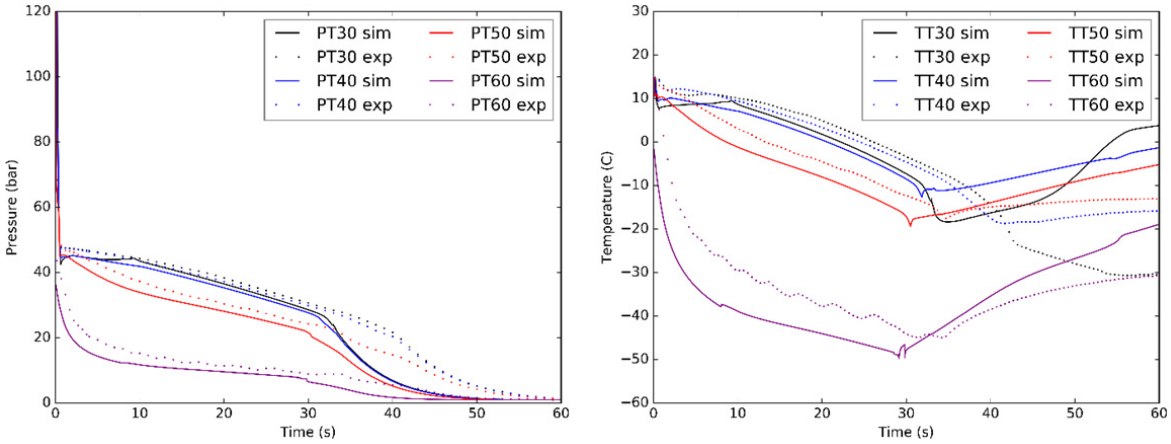

Figure 9: Experimental and SINTEF code pressure and temperature profiles for test 3.

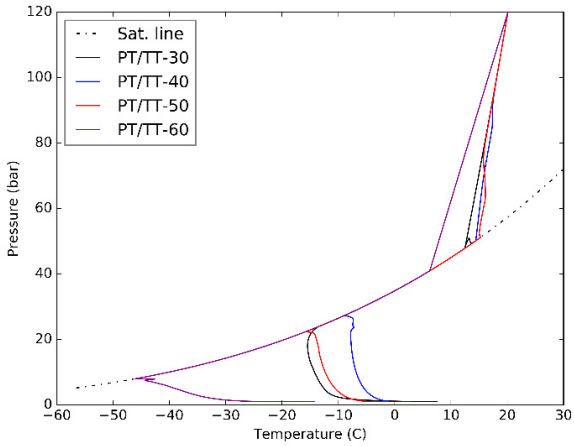

Figure 10: PT trajectory for the four sensors in test 1 from SINTEF code.

7. Conclusions

Pressure-release investigations have been performed in a tube filled with pure liquid CO_2. High-frequency pressure and temperature sensors were employed in order to measure the effect of the choked flow through the orifice and the corresponding Joule-Thompson effect.

The results from the experimental investigations have been compared to OLGA and SINTEF Energy flow assurance tools. Overall the numerical results match the experimental results. A consistent slight underestimation of about 2-10 degrees in the predicted minimum temperature in the initial phase of the decompression was observed. This is could be caused by inaccuracies in the heat transfer correlations used at the inner wall of the pipe.

The outer heat transfer coefficient was modelled, and was found to vary significantly with the ambient air humidity and velocity, and with the surface temperature of the pipe. Nevertheless, a constant value of 55 W/(m2K) was used in the simulations. Since neither air humidity nor air velocity was measured, there is some uncertainty related to the magnitude of the heat transfer from the ambient to the pipe.

Used simulation models have certain complexity, but still contain several simplifications. In view of this, the relatively good results, particularly for pressure, are encouraging. Further development of SINTEF Energy tool could include more advanced heat-transfer models taking into account the effect of boiling and flow regimes. In addition, further experimental investigations could be executed using improved temperature sensors which are more sensitive to the occurring temperature drop during pressure release. This will probably reduce the absolute discrepancies observed between the numerical and experimental results.

Acknowledgements

The modelling work was performed in the Demonstration of Flow Assurance for CO_2 Transport Operations (DeFACTO) project. The authors acknowledge the support from the Research Council of Norway, CLIMIT Demo (227680)

References

[1] de Koeijer, G., Hammer, M., Drescher. M. and Held, R., Need for experiments on shut-ins and depressurizations in CO2 injection wells. Energy Procedia 2014, **63**: 3022-3029.
[2] Munkejord, S.T., Hammer, M. and Løvseth, S.W. CO2 transport: Data and models – A review, Applied Energy 2016, **169**:499-523.
[3] Armstrong, K. and Allason D. 2" NB shocktube releases of dense phase CO2. Tech. rep., GL Noble Denton, Gilsland Cumbria, UK, 2014. URL https://www.dnvgl.com/oilgas/joint-industry-projects/ongoing-jips/co2pipetrans.html
[4] Drescher, M., Varholm, K., Munkejord, S.T., Hammer, M., Held, R. and de Koeijer, G. Experiments and modelling of two-phase transient flow during pipeline depressurization of CO2 with various N2 compositions, Energy Procedia 2014, **63**:2448-2457.
[5] Frank Kreith & William Z. Black, Basic Heat Transfer, 1980, ISBN 0-700-22518-8
[6] Håvelsrud, M. Improved and verified models for flow of CO_2 in pipelines, The Third International Forum on the Transportation of CO_2 by Pipeline, Clarion Technical Conferences, Gateshead, UK, 2012.
[7] Span, R. and Wagner, W. A new equation of state for carbon dioxide covering the fluid region from the triple-point temperature to 1100 K at pressures up to 800 MPa, J. Phys. Chem. Ref. 1996, **25**(6): 1509-1596
[8] Jäger, A. and Span, R. Equation of state for solid carbon dioxide based on the Gibbs free energy. J. Chem. Eng. Data, 2012, **57**:590–597.
[9] Vesovic, V., W. A. Wakeham, G. A. Olchowy, J. V. Sengers, J. T. R. Watson and J. Millat. The transport properties of carbon dioxide., J. Phys. Chem. Ref. Data, 1990, **19**:763.
[10] Fenghour, A. and Wakeman, W. A. The viscosity of carbon dioxide. J. Phys. Chem. Ref. Data, 1998, **27**:31-44.
[11] Rathjen, W. and Straub, J. Temperature dependence of surface tension, coexistence curve, and vapor pressure of CO2, CClF3, CBrF3, and SF6. [book auth.] E. Hahne and U. Grigull. Heat Transfer in Boiling. New York : Taylor & Francis Inc., 1977, **18**:425-451.
[12] Munkejord, S.T. and Hammer, M. Depressurization of CO2-rich mixtures in pipes: Two-phase flow modelling and comparison with experiments, International Journal of Greenhouse Gas Control 2015, **37**:398-41.
[13] Aursand, E., Dumoulin, S., Hammer, M., Lange, H.I., Morin, A., Munkejord, S.T. and Nordhagen, H.O. Fracture propagation control in CO2 pipelines: Validation of a coupled fluid–structure model, Engineering Structures 2016, **123**:192-212.